Original Article

Assessment of Cytotoxicity and Odontogenic/Osteogenic Differentiation Potential of Nano-Dentine Cement Against Stem Cells from Apical Papilla

Eshagh Ali Saberi, M.D.S.[1], Narges Farhad Mollashahi, M.D.S.[1], Fatemeh Ejeian, M.Sc.[2], Marzieh Nematollahi, M.Sc.[2], Omolbanin Shahraki, Ph.D.[3], Arezoo Pirhaji, M.D.S.[4*], Mohammad Hossein Nasr-Esfahani, Ph.D.[2*]

1. Department of Endodontics, Faculty of Dentistry, Oral and Dental Diseases Research Center, Zahedan University of Medical Sciences, Zahedan, Iran
2. Department of Animal Biotechnology, Cell Science Research Center, Royan Institute for Biotechnology, ACECR, Isfahan, Iran
3. Pharmacology Research Center, Zahedan University of Medical Sciences, Zahedan, Iran
4. Department of Endodontics, Faculty of Dentistry, Zahedan University of Medical Sciences, Zahedan, Iran

Corresponding Addresses: P.O.Box: 9817699693, Department of Endodontics, Faculty of Dentistry, Zahedan University of Medical Sciences, Zahedan, Iran
P.O.Box: 8159358686, Department of Animal Biotechnology, Cell Science Research Center, Royan Institute for Biotechnology, ACECR, Isfahan, Iran
Emails: arezoo.pirhaji.ap@gmail.com, mh.nasr-esfahani@royaninstitute.org

Received: 04/July/2021, Accepted: 24/January/2022

Abstract

Objective: Assessment of the cytotoxicity of novel calcium silicate-based cement is imperative in endodontics. This experimental study aimed to assess the cytotoxicity and odontogenic/osteogenic differentiation potential of a new calcium silicate/pectin cement called Nano-dentine against stem cells from the apical papilla (SCAPs).

Materials and Methods: In this experimental study, the cement powder was synthesized by the sol-gel technique. Zirconium oxide was added as opacifier and Pectin, a plant-based polymer, and calcium chloride as the liquid to prepare the nano-based dental cement. Thirty-six root canal dentin blocks of human extracted single-canal premolars with 2 mm height, flared with #1, 2 and 3 Gates-Glidden drills were used to prepare the cement specimens. The cement, namely mineral trioxide aggregate (MTA), Biodentine, and the Nano-dentine were mixed according to the manufacturers' instructions and applied to the roots of canal dentin blocks. The cytotoxicity and odontogenic/osteogenic potential of the cement were evaluated by using SCAPs.

Results: SCAPs were characterized by the expression of routine mesenchymal cell markers and differentiation potential to adipocytes, osteoblasts, and chondrocytes. Cement displayed no significant differences in cytotoxicity or calcified nodules formation. Gene expression analysis showed that all three types of cement induced significant down-regulation of *COLA1*; however, the new cement induced significant up-regulation of *RUNX2* and *SPP1* compared to the control group and MTA. The new cement also induced significant up-regulation of TGFB1 and inducible nitric oxide synthase (iNOS) compared with Biodentine and MTA.

Conclusion: The new Nano-dentin cement has higher odontogenic/osteogenic potential compared to Biodentine and MTA for differentiation of SCAPs to adipocytes, osteoblasts, and chondrocytes.

Keywords: Biodentine, Calcium Silicate, Mineral Trioxide Aggregate, Stem Cells

Cell Journal(Yakhteh), Vol 24, No 11, November 2022, Pages: 637-646

Citation: Saberi EA, Farhad Mollashahi N, Ejeian F, Nematollahi M, Shahraki O, Pirhaji A, Nasr-Esfahani MH. Assessment of cytotoxicity and odontogenic/osteogenic differentiation potential of nano-dentine cement against stem cells from apical papilla. Cell J. 2022; 24(11): 637-646. doi: 10.22074/cellj.2022.8126.

Introduction

Different types of cement have been traditionally applied for sealing the pulp cavity and preventing bacterial leakage as an efficient vital pulp therapy (1). Although, there is still high demand for applying advanced materials in the apical region of the root canal through endodontic regeneration procedures in the hope of improving the healing process of periodontal tissues. The ultimate goal of developing novel biomaterials is to enhance their capability for inducing differentiation of mesenchymal stem cells (MSCs) to odontoblast-like cells and stimulating hard tissue formation. Indeed, the biocompatibility of these types of cement is of great importance regarding their direct contact with live tissues (2) .

Currently, mineral trioxide aggregate (MTA) is known as the most commonly used capping biomaterial in clinical studies (1), which is composed of tiny hydrophilic particles that are allowed to set in aqueous/moisture conditions (3). MTA presents suitable biocompatibility, radiopacity, and strength, which provides significant advantages in contrast to amalgam and super-EBAn (4). The optimum working time for MTA is around 5 minutes, with a setting time of 2.45 to 4 hours. Based on the literature, its cementogenesis property is attributed to the release of calcium ions reacting with phosphate groups in interstitial fluid and forming hydroxyapatite on the surface (5). However, long setting time, low compressive strength, and low flowability are considered the significant drawbacks of MTA (6). Furthermore, the ability of MTA to support the adhesion, proliferation, and anchoring of human MSCs has been previously investigated (7).

The other extensively used compound applied as

a restorative dentin replacement is Biodentine (8). It has notable superiorities over MTA, including easy manipulation, compatibility, and appropriate setting time. The major components of Biodentine are tri- and di-calcium silicate, which are incorporated with calcium carbonate, oxide fillers, and iron oxide to confer optimal color. Also, it contains calcium chloride as an accelerator, a water-soluble polymer as a dehydrator, and zirconium oxide (in some instances) as an opacifier. The preparation process of Biodentine includes a primary setting time of around 6 minand a final setting time of 10-12 minutes, which are shorter than glass ionomer and MTA (9). Over its suitable biocompatibility, Biodentine has been known as a bioactive material which promotes osteogenic differentiation and mineralization of different MSC types. It also possesses a suitable potential for inducing odontogenic differentiation and changing the equilibrium from inflammation to regeneration via decreasing the expression and activity level of TNF-induced transient receptor potential ankyrin1 (TRPA1) (10).

On the other hand, Youssef et al. (11) provided significant evidence for the cytotoxic effect of Emdogain, MTA, Biodentine, and calcium hydroxide against human dental pulp stem cells. In addition, another calcium silicate-based material (TheraCal) showed decreased proliferation rate in pulp fibroblasts and stimulated the release of IL-8 as a pro-inflammatory cytokine (12). Indeed, Saberi et al. (13) showed that the viability of stem cells from the apical papilla (SCAPs) treated with Biodentine was decreased over time.

Despite the remarkable merits of Biodentine, its high cost leads scientists to develop new inexpensive cement with improved sealability, minimized cytotoxicity, and higher osteoinductivity. In this regard, we take advantage of nano-calcium silicate and pectin biopolymer to overcome physical and chemical shortcomings faced by traditional calcium silicate cement. In addition, it was endorsed that nanomaterials revealed a higher antibacterial effect and better root canal filling (14).

Regarding the relatively low cost, renewability, diverse structures, and different physical properties, biomaterials reached many interests for use in a wide range of pharmaceutical and biomedical applications. Notably, some influential biopolymers have been developed recently with suitable applications in wound healing. They revealed a good potential for absorbing a high volume of water from the inflamed tissues when applied in dry form and providing the required water for the tissue when used in hydrated format (15). In particular, Pectin is known as a biopolymer with a wide range of biomedical activities, including B-lymphocyte activation and inducing the release of pro-inflammatory cytokines (such as IL-1B) from macrophages. Also, pectin-based materials were extensively used in traditional wound healing/dressing products, according to their noteworthy physico-chemical characteristics (16). Namely, Pectin have a suitable hydrophilicity, allowing exudate removal from the inflamed tissues (17). Also, Pectin can potentially preserve the wound site's acidic pH, which serves as a barrier against bacteria and fungi. Moreover, it could bond to various active molecules and protect them against degradation (18). Although, it is worth mentioning that there is some evidence showing the remarkable cytotoxicity of Pectin at high concentrations (19).

Despite the promising potential of Pectin as a part of the capping agent, there is no report on the evaluation of cytotoxicity and odontogenic/osteogenic differentiation potential of pectin-containing materials. So, in this research, we introduced a new calcium silicate-based cement containing pectin polymer and aimed to assess its cytotoxicity and odontogenic/osteogenic differentiation potential over SCAPs through *in vitro* condition

Materials and Methods

Synthesis and preparation of the new cement

The new cement was composed of a powder phase and a liquid phase. Generally, the powder contained 80% tri- and di-calcium silicate, 14.9% calcium carbonate (Merck, Germany) as the filler, and 5% zirconium oxide (Merck, Germany) as the opacifier, and 0.1% pectin (Sigma Aldrich, Steinheim, Germany). The tri- and di-calcium silicate was synthesized by the sol-gel technique. For this purpose, 8.48 ml of tetraethyl orthosilicate (pure TEOS, FlukaMerck, Germany) was dissolved in double distilled water, and the pH of the solution was adjusted to 4.5 by nitric acid. Then 26.58 g calcium nitrate tetrahydrate (Merck, Germany) was gradually added to the solution during continuous stirring. Next, the solution was heated at 70°C for 24 hours to form a gel (20), and the obtained gel was then heated at 120°C for 24 hours for drying. Finally, the obtained compound was heated at 1500°C for 2 hours for calcination (21). The final liquid contained, the cement was prepared by mixing the powder (0.3 g) and liquid (calcium chloride (Merck, Germany) in a capsule using an amalgamator.

Characterization of the nano-dentine

The morphological feature of raw new cement was analyzed by using scanning electron microscopy (SEM, KYKY, EM-3900M, China). Also, the crystalline structure of nano-dentine was characterized using X-Ray diffraction (XRD, Bruker D8 Advance Diffractometer) with the 2-theta method (range 5° -80°, step size 0.02°, 1 s/step). Peaks were compared with standard XRD profiles obtained from the powder diffraction file (PDF) database. ATR-FTIR spectra of cement have been collected with a Bruker Tensor II FTIR System (Bruker Optics, Ettlingen, Germany) over wavelengths between 400 cm^{-1} and 4000 cm^{-1} with a resolution of 1.5 cm^{-1}. To analyze Nano-dentine's degradation rate, the modified ANSI/ADA Specification Number 9 was applied. Briefly, hardened samples with 10 mm diameter and 1 mm thickness (n=5) were immersed in 50 ml of HPLC grade water and incubated at 37˚C for 5 and 30 days. At each time point, cement were removed, and water left to evaporate

at 80˚C following an overnight at 110˚C. Finally, the residual materials were collected, and the weight loss percentage was calculated based on the formulation of ΔW%=[(W2-W1)/W1]*100, through which W1 indicating the weight of the initial dried material and W2 referred to the material weight at the end of incubation time points.

Application of cement into root canal dentine blocks

Human single-rooted premolars were taken from teeth extracted for various clinical reasons (as part of prosthetic, periodontal, or orthodontic treatment) following obtaining written informed consent from the patients. The study was approved by the ethics committee of Zahedan University of Medical Sciences (IR.ZAUMS.REC.1398.353). All teeth underwent digital periapical radiography in buccolingual and mesiodistal directions. The teeth had mature apices, one straight canal, no history of previous endodontic treatment, and no defects such as calcification, resorption, or cracks were picked for further experiments. The hard and soft tissue residues were removed from the tooth surface using an ultrasonic scaler. After primary disinfection of the teeth with 5.5% sodium hypochlorite for 10 minutes, and subsequent rinse with saline, they were stored in 0.9% saline until use. The teeth were then decoronated at their cementoenamel junction by a carbon disc and surgical handpiece under water coolant. A #20 K-file was used to negotiate the canal orifice. To standardize the internal canal space to have 1.5 mm diameter, #1, 2 and 3 Gates-Glidden drills were used orderly for primary flaring of the canal. Subsequently, final root canal preparation was performed using #2, 3, 4, and 5 peeso reamers.

Afterward, 36 roots were sectioned into dentine blocks with 2 mm height by a carbon disc and surgical handpiece under water coolant. The specimens were then stored in 0.9% saline, randomly divided into 3 groups (n=12 for each), and sterilized at 121°C and 2 bar pressure for 20 minutes. MTA and Biodentine were prepared according to the manufacturers' instructions in aseptic conditions and packed in the root canal of the dentine block. Briefly, the powder and liquid were homogenously mixed in 1:3 ratios to prepare MTA. For Biodentine, five drops of the liquid part were added to each capsule and underwent trituration in an amalgamator at 4000 rpm for 30 seconds to achieve a paste-like consistency. In the case of new cement, six drops of the liquid were added to each capsule and mixed in an amalgamator at 4000 rpm for 15 seconds until obtaining a paste-like consistency. Finally, all specimens were incubated in a moist environment for 15 minutes for the primary setting. The sample preparation procedure was schematically presented in Figure 1A.

Cell isolation and culture

As previously reported, the SCAPs were harvested and characterized from healthy immature human third molar teeth (22). The teeth were extracted for other medical issues after obtaining informed consent from volunteers. Briefly, the apical tissue was rinsed with phosphate buffered saline (PBS, Bio-Idea, Tehran, Iran) supplemented with penicillin-streptomycin (2X Penicillin-Streptomycin, Gibco, Paisley, UK). For enzymatic digestion, first, the apical tissue was diced into pieces by a surgical scalpel, and the pieces were exposed to 3 mg/mL of collagenase type I and 4 mg/mL dispase (both from Gibco, Paisley, UK) for 30 to 45 minutes at 37°C. Next, the obtained cell suspension was filtered through a 70-µm filter mesh and centrifuged for 8-10 minutes at 1800 rpm. The collected cells were cultured in minimum essential Eagle's medium (a-MEM, Sigma, Munich, Germany), supplemented with 15% fetal bovine serum (FBS, Gibco, Paisley, UK), 1% Glutamax, 1% penicillin/streptomycin, 250 µg/mL amphotericin B (PAA, Cölbe, Germany), and gentamycin (Gentamicin Sulfate, Sigma, Munich, Germany), then incubated (Labotec C200) at 37°C and 5% CO_2 and filling the dish, the cells were passaged after reaching confluence condition.

Characterization of isolated cells

To evaluate the stemness of the isolated cells, expression of CD105, CD45, CD146, CD73, STRO-1, and CD90 surface markers was measured by flow cytometry. For this purpose, after counting the cells, they were fixed in 4% paraformaldehyde at 4°C for 30 minutes and permeabilized using 0.2% Triton-X100 for 30 minutes. The fixed cells were then rinsed with PBS and incubated in primary antibodies (all from Merck Millipore, Billerica, MA, USA) diluted in 10 mg/mL BSA overnight. Finally, the following incubation with appropriate secondary antibodies at 37°C for 2 hours, the expression analysis was performed by a FACS Calibur cytometer (Becton Dickinson, San Jose, CA, USA) and analyzed by WinMDI 2.9 software.

Next, their three-lineage differentiation potential was evaluated. For this purpose, after reaching over 95% confluence, the culture medium was replaced with an osteogenic medium (including 0.1 µM dexamethasone, 50 µg/mL ascorbic acid-2 phosphate, and 10 mM beta-glycerophosphate), and adipogenic medium (containing 0.1 µM dexamethasone, 50 µg/mL ascorbic acid-2 phosphate and 50 µg/mL indomethacin). To induce chondrogenic differentiation, cells were centrifuged at 300 g for 5 minutes and incubated in a basic culture medium supplemented with a specific chondrogenic medium containing 0.1 µM dexamethasone, 50 µg/mL ascorbic acid-2 phosphate, 10 ng/mL transforming growth factor B (TGFB1), and 1% ITS. The medium was refreshed every 3 days for 21 days. At the end of the differentiation period, specific staining was carried out for the assessment of osteogenic differentiation (Alizarin Red S staining), chondrogenic differentiation (Toluidine Blue staining), and adipogenic differentiation (Oil Red-O staining).

***In vitro* osteogenic/odontogenic differentiation assay**

To assess the odontogenic/osteogenic differentiation of SCAPs in the presence of different blocks, cells

were cultured with a density of 2.1×10^5. After reaching 90% confluency, the culture medium was replaced with an odontogenic/osteogenic medium, as previously described in section 3.3. The efficiency of odontogenic/osteogenic differentiation was evaluated by Alizarin Red staining and analyzing the expression level of specific markers by quantitative real-time polymerase chain reaction (qRT-PCR). Each test was performed in three independent experiments, and the values were reported as mean values ± SEM.

Cytotoxicity assay

To assess the potential cytotoxicity of cement in direct contact with the SCAPs, cultured cells were faced with dentine blocks filled with cement placed on top of 6.5-mm diameter, 0.4 μm pore size transwell inserts wholly covered with the culture medium. The cultured cells without cement were evaluated as the control group. Also, the indirect cytotoxicity of cement was evaluated following incubation of cells with a medium conditioned with dentine blocks for 10 days through culture conditions.

After 1, 3, 5, 7, and 10 days, the cells' metabolic activity and proliferation rate was measured with an MTS assay using the MTS kit (Promega, USA), based on the manufacturer's instruction. Briefly, the dentine blocks were removed from the wells after 3.5 hours' incubation with MTS/PMS. The product absorbance was measured at 490 nm by a microplate reader (Fluostar Optima, BMG Lab Technologies, Germany). Each test was performed in three independent experiments, and the values were reported as mean values ± SEM.

Alizarin Red staining

After 21 days, the cells were rinsed with PBS, fixed with 96% ethanol, and stained with 0.2% Alizarin Red (pH=6.4) for 1 hour at room temperature. Eventually, cells were immersed in a solution of 20% methanol and 10% citric acid for 15 minutes. Then, the conditioned solution was transferred to 96-well plates, and their optical density was read at 450 nm using a microplate reader (Fluostar Optima, BMG Lab Technologies, Germany).

RNA extraction, cDNA synthesis, and quantitative real-time polymerase chain reaction analysis

The SCAPs were rinsed with PBS and collected in Trizol reagent (Sigma, Munich, Germany), following the differentiation process. Total RNA extraction was carried out using the phenol-chloroform method. To eliminate possible DNA contamination, the extracted samples were treated with DNase1, and cDNA was synthesized according to the protocol provided by the kit (Fermentas, CA, USA). Next, the qRT-PCR analysis was performed for specific osteogenic markers (*COL1A1, SPP1/OPN*, and *RUNX2)* as well as well-known inflammatory-related genes *(TNF-alpha*, *TGFB1*, and *iNOS)* using ABI device (Applied Biosystems, USA). Detailed information for the primers is provided in Table 1. The relative expression of the target genes was calculated through the delta-delta-Ct (ddCt) method compared to the untreated cells before differentiation induction.

Table 1: Information on primers used in quantitative real-time polymerase chain reaction

Gene symbol	Primer sequence (5´-3´)	Accession number
rh.B.actin	F: AGATGCGTTGTTACAGGAAG R: TGTGTGGACTTGGGAGAG	NM_001101.3
rh.COL1A1	F: TAGTCTGTCCTGCGTCCTCTG R: TTTTGCTTCCTCCCACCCCTA	NM_000088.3
rh.SPP1	F: TTCGCAGACCTGACATCCA R: CCATTCAACTCCTCGCTTTCC	NM_001251830.1
rh.TNF-alpha	F: TAAGAGGGAGAGAAGCAACT R: CAGTATGTGAGAGGAAGAGAAC	NM_000594.3
rh.RUNX2	F: TCACTGCCTCTCACTTGCCA R: TACACACATCTCCTCCCTTC	NM_001015051.4
rh.TGFB1	F: ACAATTCCTGGCGATACCTCA R: GTGAACCCGTTGATGTCCACT	NM_000660.5
rh-iNOS	F: GTCCCCTTTCTACTACTATC R: CTGATTTTCCTGTCTCTGTC	NM_000625.4

Statistical analysis

The data were analyzed using SPSS version 16 (Inc., Chicago, USA) via one-way ANOVA and t test. $P<0.05$ were considered significant.

Results

Characterization of new cement

The macroscopic appearance of new cement revealed a white powder (Fig.1A) composed of relatively homogeneous grain size, as shown in SEM images (Fig.1B, C). Moreover, the X-ray diffraction peaks for the Nano-dentine has properly matched the standard graphs for Ca_3SiO_5 (reference ID: 14-0693) and Ca_2SiO_4 (reference ID: 31-0297), which confirmed the presence of the crystalline form of calcium silicates, as the main component of the Nano-dentine (Fig.1D, E).

The transmission spectrum of nano-dentine cement showed a peak at 512 cm^{-1} attributed to the vibration bending of calcium silicate anhydrate (SiO_4^{2-}), which was also observed in biodentine and MTA spectrum (Fig.1F). For both nano-dentine and biodentine, the strong band around 1460 cm^{-1} could be assigned to the aromatic ring, and the weak peak at 712 cm^{-1} ascribed to the V_4 vibrations of CO_3. Moreover, the sharp peak around 870 cm^{-1} in all types of cement is associated with the C-O group. The biodegradation assay revealed an increasing rate of degradation, through which the mean cumulative weight loss (%) of Nano-dentine after 5 and 30 days were 6.16% ± 0.47 and 11.13 % ± 0.75, respectively.

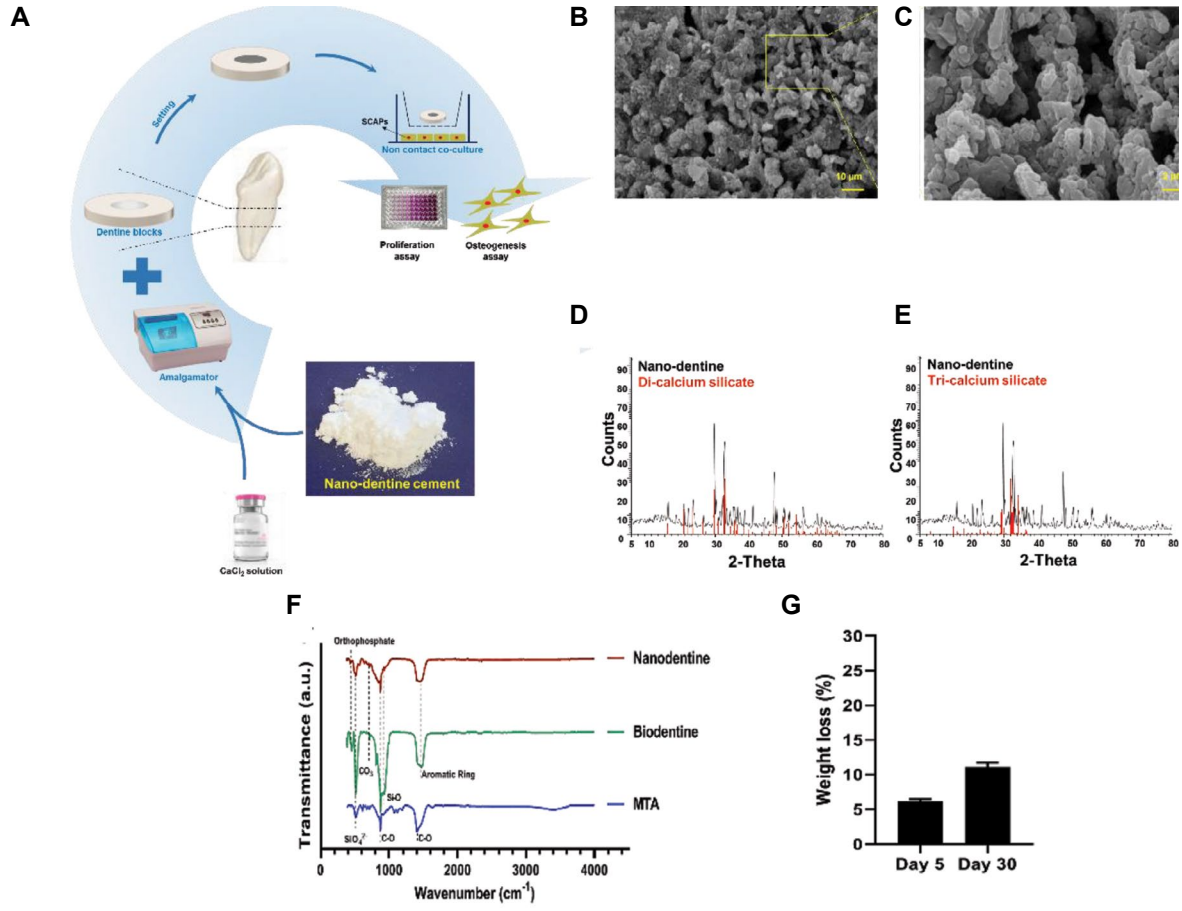

Fig.1: Characterization of Nano-dentine cement. **A.** The schematic presentation of experimental design. Scanning electron microscopic images of the cement at the magnification of **B.** 100X, and **C.** 500X. XRD diffraction pattern of Nano-dentine compared to the standard patterns of **D.** Di-calcium silicate and **E.** Tri-calcium silicate. **F.** FTIR spectrum of three MTA, Biodentine, and Nano-dentine in the wave range of 400-4000 cm^{-1}. **G.** The weight loss percentage of Nano-dentine cement over five and 30 days. Results from three independent experiments are expressed as means ± SEM. XRD; X-ray diffraction, FTIR; Fourier transform infrared, and MTA; Mineral trioxide aggregate.

Isolation of SCAPs

After 48 hours from the primary seeding, adhered cells colonies appeared, which covered almost 70% of the culture plate following 10 days' incubation in normal culture conditions (Fig.2A). The cells resembled fibroblast-like morphology and grew as a monolayer after the first passage (Fig.2B). After the three passages, we reached a relatively homogenous population of stem cells used for further characterization.

Assessment of the expression of mesenchymal stem cell markers by flow cytometry

The expression of specific mesenchymal stem cell markers, including CD146, STRO-1, CD105, CD90, and CD73,and a hematopoietic stem cell marker (CD45) at passage 4 revealed a substantial expression of all MSC-related markers. Figure 2C exhibited a representative histogram for each protein approved that over 95% of the cells expressed mesenchymal cell markers (CD73, CD90, CD105), and around 90% of the cells expressed dental stem cell markers (CD146, STRO-1). However, the cells did not express CD45 as a prominent hematopoietic stem cell marker (0.45%).

Assessment of differentiation potential of cells into three mesenchymal cell lines

Staining with Oil Red, Alizarin Red, and toluidine blue after 21 days of treatment in the specific media confirmed the differentiation potential of isolated cells to adipocytes, osteoblasts, and chondrocytes, respectively (Fig.2D-F). The lipid particles formed in adipocytes colored red after Oil Red staining (Fig.2D). Also, calcium-phosphate deposits released from osteoblasts completely covered the cell surface and appeared in the form of red nodules after Alizarin Red staining (Fig.2E). After sectioning the formed cartilaginous masses and their staining with toluidine blue, the underlying collagen in the ECM of chondrocytes in lacuna-shaped structures confirmed the formation of cartilage-like tissue (Fig.2F).

Assessment of proliferation and viability of SCAPs

Assessment of proliferation rate of the cells directly or indirectly faced with different dentine blocks via MTS assay revealed no significant difference in cell viability during 10 days. The results indicated an increasing profile in metabolic activity for all experimental groups over time. Whenthe cells were directly treated with Nano-dentine, they showed maximum cell viability and proliferation rate on the day 7,

similar to the control group. However, MTA and Biodentine groups reached maximum absorbance after 10 days (Fig.3A). Although the MTA-conditioned medium caused higher cellular metabolic activity in all time points, significant differences were only observed against Biodentine on day 3 and day 10, as well as Nanodentine on day 3 (Fig.3B).

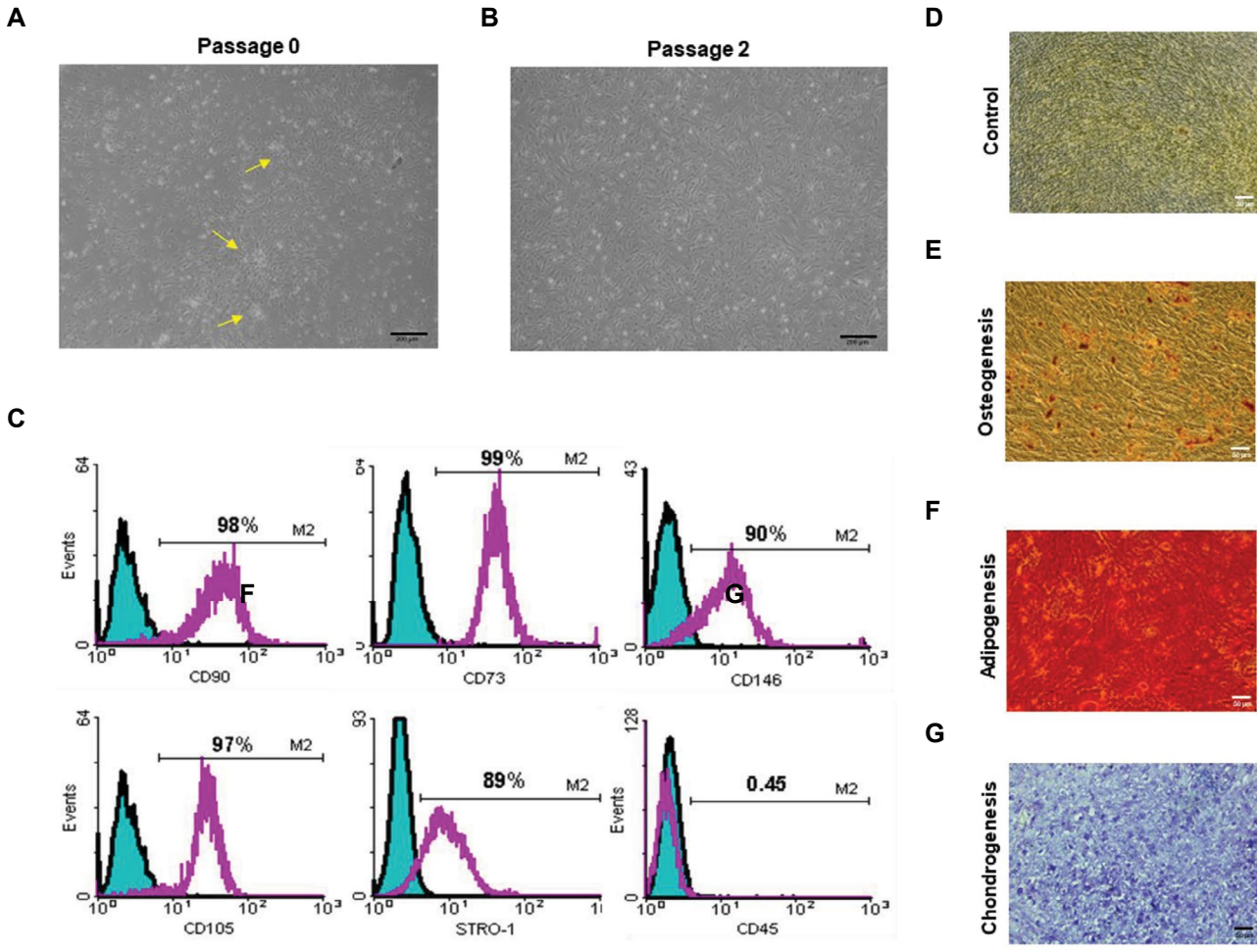

Fig.2: Characterization of harvested cells from apical papilla. Inverted microscopic photographs of the morphology of SCAPs. **A.** 10 days after primary culture. Colonies formed in the primary culture are marked with yellow arrows, **B.** After the second passage (scale bar=200 µm). **C.** Representative histogram of the expression of CD105, CD90, CD73, CD146, STRO-1, and CD45. Green histogram indicates cell fluorescence with the control antibody (isotype control), and a purple histogram indicates cell fluorescence with the respective antibody. **D.** Control cells following 21 days of cultivation under normal culture conditions. Assessment of multilineage differentiation potential of isolated cells to **E.** Adipocytes, **F.** Osteoblasts, and **G.** Chondrocytes after 21 days of treatment in specific media, and stained with Oil Red, Alizarin Red, and toluidine blue, respectively. SCAPs; Stem cells from apical papilla.

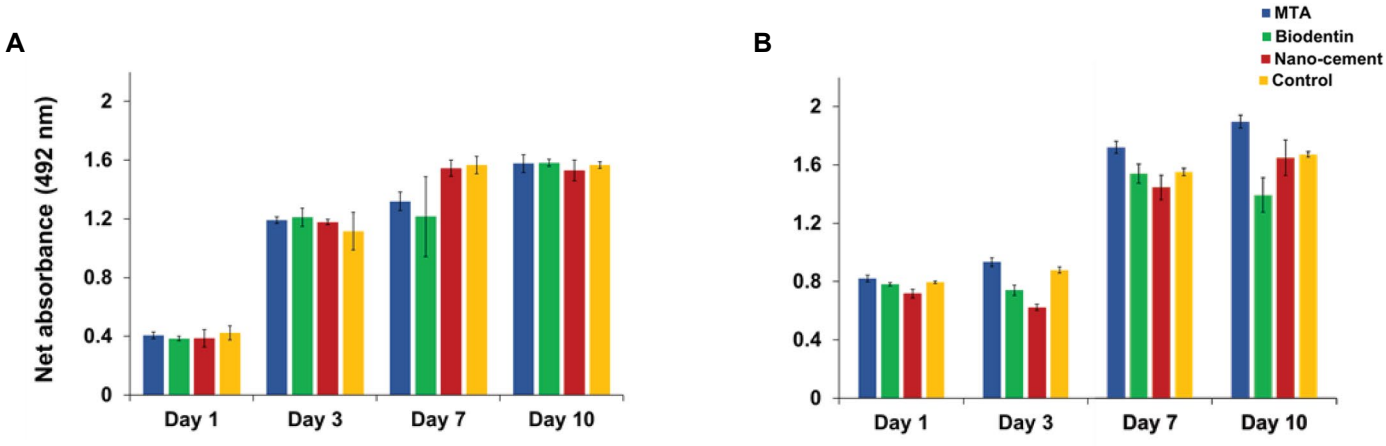

Fig.3: Assessment of the viability of SCAPs using the MTS assay. The absorbance of formazan at 492 nm wavelength at 1, 3, 7, and 10 days after culture indicated the activity and viability of cells **A.** Directly or **B.** Indirectly treated with the Nano-dentine cement, MTA and Biodentine, compared with the no-cement control groups. Data are presented as the mean value of three independent experiments ± SEM. SCAPs; Stem cells from apical papilla, MTS; 3-(4,5-dimethylthiazol-2-yl)-5-(3-carboxymethoxyphenyl)-2-(4-sulfophenyl)-2H-tetrazolium, and MTA; Mineral trioxide aggregate.

Assessment of odontogenic/osteogenic differentiation by real-time qRT-PCR

Analyzing the expression value of odontogenic/osteogenic markers at the mRNA level in the treated cells, compared with pre-incubation cells revealed significant down-regulation of *COLA1* simultaneous with significant up-regulation of *RUNX2* and *SPP1* as indicators of bone specification and osteoblast maturation, respectively, in all samples. Significant up-regulation of these markers was particularly noted in the new cement group, compared with the control and MTA groups (P=0.01, Fig.4A-C).

Assessment of osteogenic differentiation by Alizarin Red staining

Semi-quantitative analysis of Alizarin Red S accumulation revealed no significant differences (P>0.05) in calcium deposition between SCAPs exposed to different cements after 21 days treatment with osteogenic medium. In addition, neither the Nano-dentine nor the commercial counterparts (Biodentine and MTA) showed significant difference compared with the control group (Fig.4D, E).

Assessment of the expression of markers involved in inflammation by real-time qRT-PCR

No sign of up-regulation of pro-inflammatory markers (inducible nitric oxide synthase (iNOS) and TNF-alpha) was observed after 21 days of treatment with Biodentine and MTA in comparison to control. However, SCAPs exposed to the new cement showed relative up-regulation of both markers. On the other hand, expression of TGFB1 increased in all experimental groups, particularly in the new cement group (Fig.5).

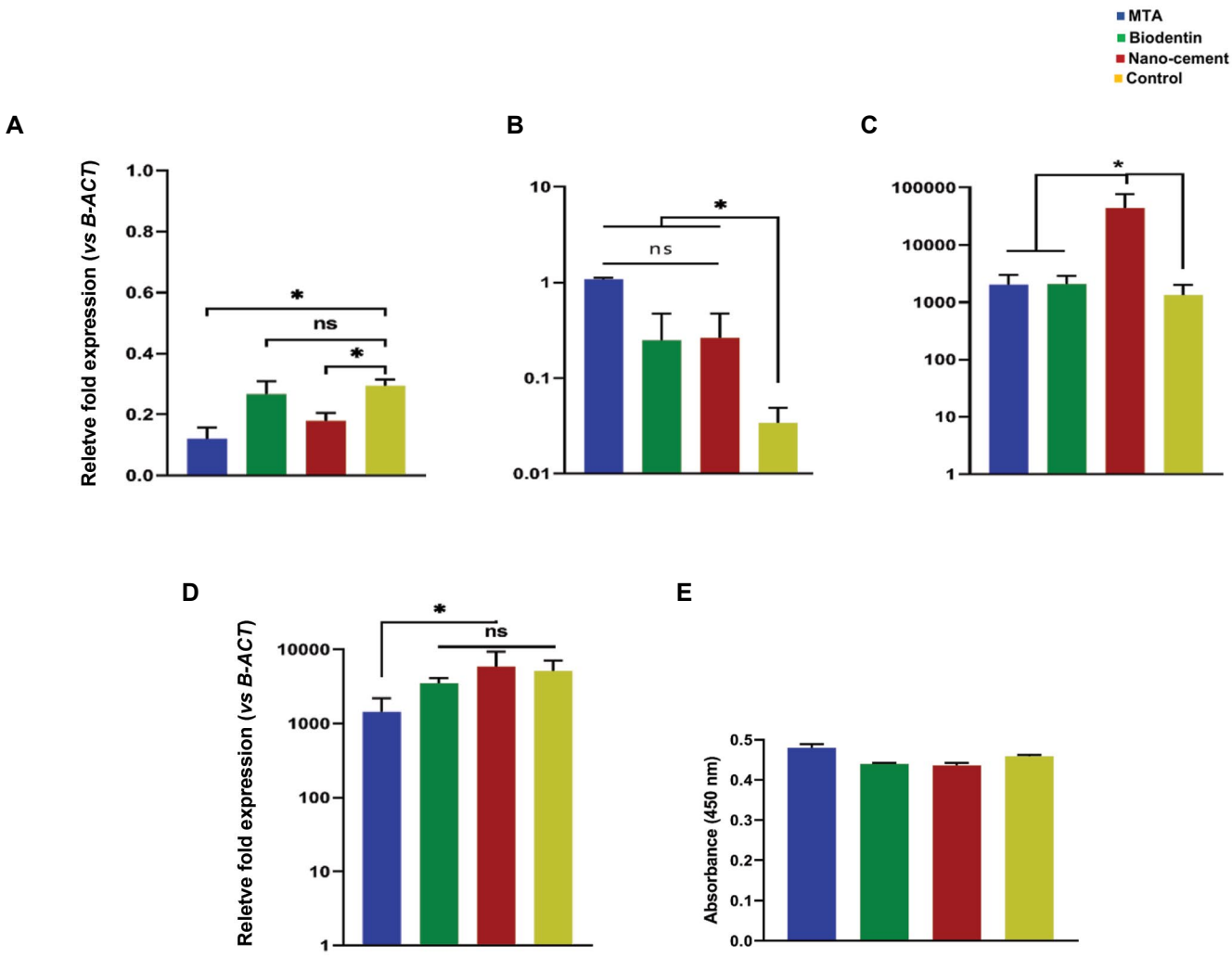

Fig.4: Assessment of the osteogenic potential in the presence of dental materials. Analysis of the mRNA expression level of **A.** *ALP*, **B.** *COLA1*, **C.** *RUNX2*, and **D.** *SPP1* as the indicators of early, intermediate, and maturation phase of osteoblasts compared with their expression before induction of differentiation (day 0). Data are presented as the mean value of three independent experiments ± SEM. **E.** Semi-quantitative analysis of Alizarin Red staining in different groups using spectrophotometry at 450 nm wavelength. Data are presented as the mean value of three independent experiments ± SEM. *; Indicates a significant difference with P<0.05 and ns; Non significant change.

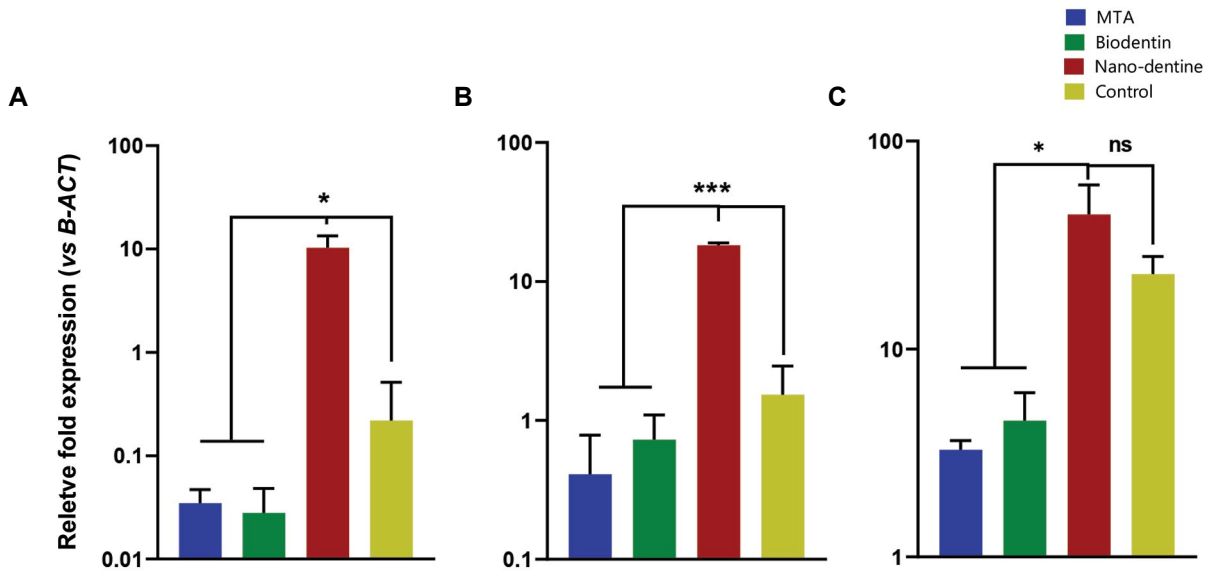

Fig.5: Expression of markers involved in inflammation at the mRNA level. Expression of **A.** TNF-alpha and **B.** iNOS as markers of Inflammation, and **C.** TGFB1 as an anti-inflammatory marker, compared with their expression before induction of differentiation (day 0). Data are presented as the mean value of three independent experiments ± SEM. * indicates a significant difference with *; P<0.5, ***; P<0.005, TNF; Tumor necrosis factor, iNOS; Inducible nitric oxide synthase, and ns; Non significant change.

Discussion

In this study, we introduced Nano-dentine as a novel calcium silicate-based material and assessed its bio-functionality against SCAPs. We found that SCAPs could survive and proliferate in the presence of dentine blocks filled with the Nano-dentine similar to the control group and the commercial counterpart (MTA and Biodentine). The SCAPs have reached a steady state after seven days, while maximum cell proliferation in MTA and Biodentine groups were reported on day ten post treatment. The higher proliferation rate of cells in the presence of Nano-dentine is likely attributed to the pectin component. Pectin isa natural water-soluble polymer, which is widely used in food and drink manufacturing industries as a concentrating, reinforcing, and gelation reagent. In addition, there are numerous reports on the significant antiproliferative effect of Pectin on cancer cells via inducing apoptosis or regulating cell signaling pathways (23). It is evident that Pectin only has an inhibitory effect on cells that express the galectin receptor, especially in high concentrations (24). Intravenous injection of Pectin also triggered coagulation in a shorter time which would be beneficial for controlling hemorrhage and local bleeding (25). Pectin's physicochemical properties highlightedits relevance for wound dressing and elimination of exudates from the wound site (17).

In addition, Pectin can prevent the colonization of bacteria and fungi by providing the acidic pH in the environment and protecting biomaterials against degradation via binding active sites (18). Nano-dentine revealed a suitable degradation rate after one week (7.33%) comparable to Portland cement as well as gray and white MTA (26).

Furthermore, our findings align with previous reports on reasonable cytotoxicity of Biodentine and MTA over SCAPs (13, 27). Although Nano-dentine group showed a higher level of *RUNX-2* and *SPP1* expression, *COLA1* was expressed in a similar way in all experimental groups, which was probably due to the high primary level of *COLA1* in dental-related stem cells (28). It is evident that the expression level of *ALP*, as an early marker of osteogenesis, was reduced in all groups at the end of treatment time. This finding is in harmony with the highly overexpression of *SPP1*, as a late osteogenic marker, and confirms the maturity of osteoblasts. In this way, alizarin red staining confirmed the functional osteoblast differentiation in all experimental groups, which is consistent with the previous report on the remarkable calcification induced by MTA and Biodentine due to the release of calcium hydroxide and deposition of hydroxyapatite (27).

RUNX2 is a key transcriptional modulator for osteoblastic differentiation, which plays a critical role in the maturation and homeostasis of osteoblasts during embryogenesis and regeneration (29). Indeed, *SPP1* (osteopontin) which is known as the critical non-collagenous bone matrix phospho-glycoprotein, reveals a high affinity to hydroxyapatite and acts as a chemo-attachment for osteoclasts (30). Hence, it is directly and actively involved in the process of bone resorption by osteoclasts (31, 32).

Moreover, the SCAPs showed a significantly higher expression level of TNF-alpha, TGFB1, and iNOS after exposure to Nano-dentine compared to Biodentine and MTA. This effect may be attributed to the positive impact of Pectin on the expression/ activation of SMAD3 as the main effector of the TGFB signaling pathway (33). Additionally, Amorimet al. (34) showed that this biopolymer i increases NOS expression. A different

line of studies has asserted that in natural dentine tissue, odontoblast express pro- and anti-inflammatory cytokines having paracrine/autocrine effect (35). A complex orchestration of inflammatory mediators seems to be required for the regeneration process. In this way, Saberi et al. (27) reported a significant increase in the expression of TNF-alpha after 3 and 7 days of treatment with MTA and Biodentine, respectively. It has been documented that TGFB1 plays a fundamental role in the migration and differentiation of stem cells to odontoblast-like cells (36). Also, FGF2 and TGFB1 play critical roles in the induction, specification, and morphogenesis of stem cells during odontogenesis (37).

Nitric oxide is a free radical produced from L-arginine guanidino-nitrogen in three isoforms [endothelial NOS (eNOS), neural NOS (nNOS), and iNOS], depending on the tissue origin and their physiological role (38). In particular, iNOS and eNOS are expressed by the stromal bone marrow cells, osteoblasts, osteocytes, and osteoclasts, whereas the expression of nNOS is limited to osteolineages. Although all three NOS isoforms play an important role in bone healing, iNOS is considered the main factor (39). The substantial overexpression of iNOS in Nano-dentine supports this material's higher potential for osteo-induction.

Conclusion

Getting all together, we introduce dentine blocks as a novel method for simulating the natural clinical condition. The Nano-dentine cement showed comparable results to Biodentine and MTA in the preservation of cell viability and formation of calcified nodules. Nano-dentine's sensible odontogenic/osteogenic potential was approved via up-regulation of *RUNX2*, *SPP1*, *iNOS*, *TNF-alpha*, and *TGFB1* markers, which seems to depend on the presence of Pectin in its formulation. Moreover, Nano-dentine showed some superiorities over the other materials because of easy manipulation, less setting time, and low price. These advantages lead Nano-dentine to find a broad application in vital pulp therapy (direct and indirect pulp capping, partial and cervical pulpotomy), apexification, endodontic regeneration, repair of root perforations, and root-end filling.

Acknowledgements

The authors thank all members of the Royan Institute for preparing facilities and an outstanding scientific environment during this project. There is no financial support and conflict of interest in this study.

Authors' Contributions

E.A.S., F.E., A.P.; Participated in conception and design, data evaluation, and statistical analysis. M.N., A.P.; Contributed to experimental study and data collection. O.Sh.; Performed material preparation and characterization. E.A.S.; Drafted the manuscript. F.E., N.F.M.; Analysed the results and critically revised the manuscript. A.P., M.H.N.-E.; Took the lead in writing the manuscript and supervised the research. All authors performed editing and approved the final version of this paper for submission.

References

1. Holliday R, Alani A. Traditional and contemporary techniques for optimizing root canal irrigation. Dental Update. 2014; 41(1): 51-61.
2. Gomes-Filho JE, Watanabe S, Bernabé PFE, de Moraes Costa MT. A mineral trioxide aggregate sealer stimulated mineralization. J Endod. 2009; 35(2): 256-260.
3. Shojaee NS, Sahebi S, Karami E, Sobhnamayan F. Solubility of two root-end filling materials over different time periods in synthetic tissue fluid: a comparative study. J Dent (Shiraz). 2015; 16(3): 189-194.
4. Song M, Yoon TS, Kim SY, Kim E. Cytotoxicity of newly developed pozzolan cement and other root-end filling materials on human periodontal ligament cell. Restor Dent Endod. 2014; 39(1): 39-44.
5. Roberts HW, Toth JM, Berzins DW, Charlton DG. Mineral trioxide aggregate material use in endodontic treatment: a review of the literature. Dent Mater. 2008; 24(2): 149-164.
6. Silva E, Senna P, De-Deus G, Zaia A. Cytocompatibility of Biodentine using a three-dimensional cell culture model. Int Endod J. 2016; 49(6): 574-580.
7. D'Antò V, Di Caprio MP, Ametrano G, Simeone M, Rengo S, Spagnuolo G. Effect of mineral trioxide aggregate on mesenchymal stem cells. J Endod. 2010; 36(11): 1839-1843.
8. Luo Z, Kohli MR, Yu Q, Kim S, Qu T, He W-x. Biodentine induces human dental pulp stem cell differentiation through mitogen-activated protein kinase and calcium-/calmodulin-dependent protein kinase II pathways. J Endod. 2014; 40(7): 937-942.
9. Malkondu Ö, Karapinar Kazandağ M, Kazazoğlu E. A review on biodentine, a contemporary dentine replacement and repair material. Biomed Res Int. 2014; 2014: 160951.
10. Saberi E, Farhad-Mollashahi N, Saberi M. Interaction of intracanal medicaments with apical papilla stem cells: quantitative cytotoxicity assessment by methyl thiazolyl tetrazolium, trypan blue and lactate dehydrogenase. Minerva Stomatol. 2019; 68(1): 36-41.
11. Youssef AR, Emara R, Taher MM, Al-Allaf FA, Almalki M, Almasri MA, et al. Effects of mineral trioxide aggregate, calcium hydroxide, biodentine and emdogain on osteogenesis, Odontogenesis, angiogenesis and cell viability of dental pulp stem cells. BMC Oral Health. 2019; 19(1): 133.
12. Jeanneau C, Laurent P, Rombouts C, Giraud T, About I. Light-cured tricalcium silicate toxicity to the dental pulp. J Endod. 2017; 43(12): 2074-2080.
13. Saberi EA, Karkehabadi H, Mollashahi NF. Cytotoxicity of various endodontic materials on stem cells of human apical papilla. Iran Endod J. 2016; 11(1): 17-22.
14. Hamouda IM. Current perspectives of nanoparticles in medical and dental biomaterials. J Biomed Res. 2012; 26(3): 143-151.
15. Smith AM, Moxon S, Morris G. Biopolymers as wound healing materials. Wound Healing Biomaterials, Elsevier; 2016: 261-287.
16. Inngjerdingen M, Inngjerdingen KT, Patel TR, Allen S, Chen X, Rolstad B, et al. Pectic polysaccharides from Biophytum petersianum Klotzsch, and their activation of macrophages and dendritic cells. Glycobiology. 2008; 18(12): 1074-1084.
17. Munarin F, Tanzi MC, Petrini P. Advances in biomedical applications of pectin gels. Int J Biol Macromol. 2012; 51(4): 681-689.
18. Jáuregui KMG, Cabrera JCC, Ceniceros EPS, Hernández JLM, Ilyina A. A new formulated stable papin-pectin aerosol spray for skin wound healing. Biotechnol Bioprocess Eng. 2009; 14(4): 450-456.
19. Chittasupho C, Jaturanpinyo M, Mangmool S. Pectin nanoparticle enhances cytotoxicity of methotrexate against hepG2 cells. Drug Deliv. 2013; 20(1): 1-9.
20. de Souza Balbinot G, Leitune VCB, Nunes JS, Visioli F, Collares FM. Synthesis of sol–gel derived calcium silicate particles and development of a bioactive endodontic cement. Dent Mater. 2020; 36(1): 135-144.
21. Lee BS, Lin HP, Chan JCC, Wang WC, Hung PH, Tsai YH, et al. A novel sol-gel-derived calcium silicate cement with short setting time for application in endodontic repair of perforations. Int J Nanomedicine. 2018; 13: 261-271.
22. Karamali F, Esfahani MHN, Hajian M, Ejeian F, Satarian L, Baharvand H. Hepatocyte growth factor promotes the proliferation of human embryonic stem cell derived retinal pigment epithelial cells. J Cell Physiol. 2019; 234(4): 4256-4266.

23. Bergman M, Djaldetti M, Salman H, Bessler H. Effect of citrus pectin on malignant cell proliferation. Biomed Pharmacother. 2010; 64(1): 44-47.
24. Abdel-Massih R, Hawach V, Boujaoude MA. The cytotoxic and antiproliferative activity of high molecular weight pectin and modified citrus pectin. Funct Foods Health Dis. 2016; 6(9): 587-601.
25. Kadajji VG, Betageri GV. Water soluble polymers for pharmaceutical applications. Polymers. 2011; 3(4): 1972-2009.
26. Alqedairi A, Muñoz-Viveros CA, Pantera EA, Campillo-Funollet M, Alfawaz H, Abou Neel EA, et al. Superfast set, strong and less degradable mineral trioxide aggregate cement. Int J Dent. 2017; 2017: 3019136.
27. Saberi E, Farhad-Mollashahi N, Aval FS, Saberi M. Proliferation, odontogenic/osteogenic differentiation, and cytokine production by human stem cells of the apical papilla induced by biomaterials: a comparative study. Clin Cosmet Investig Dent. 2019; 11: 181-193.
28. Sollazzo V, Palmieri A, Girardi A, Zollino I, Brunelli G, Spinelli G, et al. Osteoplant acts on stem cells derived from peripheral blood. J Indian Soc Periodontol. 2010; 14(1): 12-17.
29. Ducy P, Starbuck M, Priemel M, Shen J, Pinero G, Geoffroy V, et al. A Cbfa1-dependent genetic pathway controls bone formation beyond embryonic development. Genes Dev. 1999; 13(8): 1025-1036.
30. Ohtsuki C, Kamitakahara M, Miyazaki T. Bioactive ceramic-based materials with designed reactivity for bone tissue regeneration. J R Soc Interface. 2009; 6 Suppl 3: S349-S360.
31. Dodds RA, Connor JR, James IE, Lee Rykaczewski E, Appelbaum E, Dul E, et al. Human osteoclasts, not osteoblasts, deposit osteopontin onto resorption surfaces: an in vitro and ex vivo study of remodeling bone. J Bone Miner Res. 1995; 10(11): 1666-1680.
32. Bailey S, Karsenty G, Gundberg C, Vashishth D. Osteocalcin and osteopontin influence bone morphology and mechanical properties. Ann N Y Acad Sci. 2017; 1409(1): 79-84.
33. Cao Y, Gao X, Zhang W, Zhang G, Nguyen AK, Liu X, et al. Dietary fiber enhances TGF-β signaling and growth inhibition in the gut. Am J Physiol Gastrointest Liver Physiol. 2011; 301(1): G156-G64.
34. Amorim JC, Vriesmann LC, Petkowicz CL, Martinez GR, Noleto GR. Modified pectin from Theobroma cacao induces potent pro-inflammatory activity in murine peritoneal macrophage. Int J Biol Macromol. 2016; 92: 1040-1048.
35. Park M, Pang NS, Jung IY. Effect of dentin treatment on proliferation and differentiation of human dental pulp stem cells. Restor Dent Endod. 2015; 40(4): 290-298.
36. Smith AJ, Matthews JB, Hall RC. Transforming growth factor-β1 (TGF-β1) in dentine matrix: Ligand activation and receptor expression. Eur J Oral Sci. 1998; 106(S1): 179-184.
37. He H, Yu J, Liu Y, Lu S, Liu H, Shi J, et al. Effects of FGF2 and TGFβ1 on the differentiation of human dental pulp stem cells in vitro. Cell Biol Int. 2008; 32(7): 827-834.
38. Wang FS, Kuo YR, Wang CJ, Yang KD, Chang PR, Huang YT, et al. Nitric oxide mediates ultrasound-induced hypoxia-inducible factor-1alpha activation and vascular endothelial growth factor-A expression in human osteoblasts. Bone. 2004; 35(1): 114-123.
39. Wimalawansa SJ. Nitric oxide and bone. Ann N Y Acad Sci. 2010; 1192(1): 391-403.